Inorg. Chem. **2007**, *46*, 8139–8145

Reactivity of an Adsorbed Ru(VI)–Oxo Complex: Oxidation of Benzyl Alcohol

Brooks J. Hornstein, Dana M. Dattelbaum, Jon R. Schoonover, and Thomas J. Meyer*

Los Alamos National Laboratory, Los Alamos, New Mexico 87545

Received January 11, 2007

The phosphonated ruthenium complex, $[Ru(tpy\text{-}PO_3H_2)(OH_2)_3]^{2+}$ (**1**) (tpy-PO_3H_2 = 4′-phosphonato-2,2′:6′,2″-terpyridine), was synthesized and attached to glass|ITO or glass|ITO|TiO_2 electrodes. After attachment to the metal oxide surface through the phosphonate linkage, **1** can be oxidized (either chemically or electrochemically) to the reactive Ru(VI)–dioxo complex, glass|ITO|$[((HO)_2OP)tpy)Ru^{VI}(O)_2(OH_2)]^{2+}$, which remains attached to the surface. The attached Ru(VI) complex reacts with benzyl alcohol through mechanisms similar to those proposed for the solution analog. More specifically, Ru(VI) is reduced in a stepwise fashion to Ru(IV) and then finally to Ru(II). The reduction of Ru(VI) is accompanied by a rate-limiting insertion to the C–H bond of benzyl alcohol, followed by solvolysis of the aldehyde hydrate. In addition, the surface-bound Ru(VI) acts as an electrooxidation catalyst which carries out ∼130 ($2e^-$) turnovers before deactivation.

Introduction

High-oxidation state, polypyridyl ruthenium oxo complexes are formed by oxidation and proton loss (proton-coupled electron transfer, PCET) from lower-oxidation state aqua and hydroxo precursors, for example, *cis*-$[Ru^{II}(bpy)_2(py)(H_2O)]^{2+} \xrightarrow{-e^-,-H^+}$ *cis*-$[Ru^{III}(bpy)_2(py)(OH)]^{2+} \xrightarrow{-e^-,-H^+}$ *cis*-$[Ru^{IV}(bpy)_2(py)(O)]^{2+}$(bpy = 2,2′-bipyridine, py = pyridine). The oxo complexes are potent oxidants toward a variety of organic reductants by a variety of mechanisms that have been examined in detail.[1] They are also candidates as oxidative elements in sensors and electrochemical and photoelectrochemical synthesis cells.

An extensive semiconductor attachment chemistry is available for these complexes on nanoparticle ZrO_2 and TiO_2 and other oxide surfaces based on carboxylate linkages.[2] Phosphonate linkages offer enhanced surface stability toward hydrolysis in aqueous environments.[3,4] The phosphonate linkage strategy has been used to prepare optically transparent TiO_2 nanoparticle films on glass or ITO (Sn(IV)-doped In_2O_3) electrodes containing surface-attached $[Ru^{II}(tpy)(4,4'\text{-}(PO_3H_2)_2\text{-}(bpy)(H_2O)]^{2+}$ (tpy = 2,2′:6′:2″-terpyridine; 4,4′-$(PO_3H_2)_2$-(bpy) = 4,4′-diphosphonic acid-2,2′bipyridine). UV−vis and electrochemical measurements have been used to reveal detailed mechanistic insights into the oxidation of a series of organic reductants by the attached $Ru^{IV}{=}O^{2+}$ form, glass|TiO_2-$((HO)_2OP)_2$)bpy)(tpy)$Ru^{IV}{=}O^{2+}$.[5]

We report here the application of this approach to the preparation of oxidatively active surfaces containing a four-electron, Ru(VI)−dioxo oxidant. Our strategy was to adsorb

* To whom correspondence should be addressed. E-mail: tjmeyer@unc.edu. Arey Professor of Chemistry, Department of Chemistry, University of North Carolina, Chapel Hill, NC 27599-3290.

(1) Huynh, M. H. V.; Meyer, T. J. *Inorg. Chem.* **2003**, *42*, 8140−8160 and references therein.

(2) (a) Gillaizeau-Gauthier, I.; Odobel, F.; Alebbi, M.; Argazzi, R.; Costa, E.; Bignozzi, C. A.; Qu, P.; Meyer, G. J. *Inorg. Chem*. **2001**, *40*, 6073−6079. (b) Heimer, T. A.; D'Arcangelis, S. T.; Farzad, F.; Stipkala, J. M.; Meyer, G. J. *Inorg. Chem*. **1996**, *35*, 5319−5324.

(3) (a) Gratzel, M.; Kohle, O.; Nazeeruddin, M. K.; Pechy, P.; Rotzinger, F. P.; Ruile, S.; Zakeeruddin, S. M. (Ecole Polytechnique Federale De Lausanne, Switzerland) International Patent Appl. WO 95 29, 924, Nov. 1995. (b) Pechy, P.; Rotzinger, F. P.; Nazeeruddin, M. K.; Kohle, O.; Zakeeruddin, S. M.; Humphry-Baker, R.; Graetzel, M. *J. Chem. Soc., Chem. Commun*. **1995**, *1*, 65−66. (c) Bonhote, P.; Moser, J. E.; Vlachopoulos, N.; Walder, L.; Zakeeruddin, S. M.; Humphry-Baker, R.; Pechy, P.; Graetzel, M. *Chem. Commun*. **1996**, *10*, 1163−1164. (d) Yan, S. G.; Hupp, J. T. *J. Phys. Chem*. **1996**, *100*, 6867−6870. (e) Ruile, S.; Kohle, O.; Pechy, P.; Graetzel, M. *Inorg. Chim. Acta* **1997**, *261*, 129−140. (f) Saupe, G. B.; Mallouk, T. E.; Kim, W.; Schmehl, R. H. *J. Phys. Chem. B* **1997**, *101*, 2508−2513. (g) Zakeeruddin, S. M.; Nazeeruddin, M. K.; Pechy, P.; Rotzinger, F. P.; Humphry-Baker, R.; Kalyanasundaram, K.; Graetzel, M.; Shklover, V.; Haibach, T. *Inorg. Chem*. **1997**, *36*, 5937−5946. (h) Zaban, A.; Ferrere, S.; Gregg, B. A. *J. Phys. Chem. B* **1998**, *102*, 452−460. (i) Bonhote, P.; Moser, J.-E.; Humphry-Baker, R.; Vlachopoulos, N.; Zakeeruddin, S. M.; Walder, L.; Graetzel, M. *J. Am. Chem. Soc*. **1999**, *121*, 1324−1336. (j) Trammell, S. A.; Moss, J. A.; Yang, J. C.; Nakhle, B. M.; Slate, C. A.; Odobel, F.; Sykora, M.; Erickson, B. W.; Meyer, T. J. *Inorg. Chem*. **1999**, *38*, 3665−3669.

(4) Bae, E.; Choi, W.; Park, J.; Shin, H. S.; Kim, S. B.; Lee, J. S. *J. Phys. Chem. B* **2004**, *108*, 14093−14101.

(5) Gallagher, L. A.; Meyer, T. J. *J. Am. Chem. Soc*. **2001**, *123*, 5308−5312.

10.1021/ic0700506 CCC: $37.00
Published on Web 08/25/2007

the Ru(II) precursor, $[Ru(tpy\text{-}PO_3H_2)(OH_2)_3]^{2+}$ (**1**) (tpy-PO_3H_2 = 4′-phosphonato-2,2′:6′,2″-terpyridine), followed by its electrochemical or chemical oxidation to adsorbed Ru^{VI}-(tpy-PO_3H_2)$(O)_2(OH_2)^{2+}$, ($Ru^{VI}(O)_2^{2+}$). Electrochemical and surface kinetic studies show that dioxo−Ru(VI) reactivity is retained to a remarkable degree on the surface compared to that of *trans*-$[Ru^{VI}(tpy)(O)_2(H_2O)]^{2+}$ and related Ru(VI) oxidants in solution.[6]

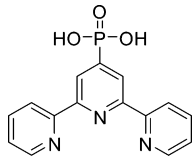

(tpy-PO_3H_2)

Experimental Section

Materials. Perchloric acid, ceric ammonium nitrate, sodium hydrogen phosphate, and sodium phosphate were purchased from Fisher Scientific and used without purification. Acetonitrile was purchased from Sigma-Aldrich and dried over activated 5 Å molecular sieves. Benzyl alcohol was also purchased from Sigma-Aldrich and stored under argon. All aqueous solutions were prepared with Millipore water (>18 MΩ). ITO electrodes were purchased from Delta Technologies, Stillwater, MN. TiO_2-coated substrates were prepared according to literature procedures and yielded films that were approximately 10 μm in thickness.[7]

[Ru(tpy-PO_3Et_2)$(C_2O_4)(OH_2)$]. [Ru(tpy-PO_3Et_2)$(C_2O_4)(OH_2)$] was synthesized by using the literature procedure for the unphosphonated tpy complex, and it was subsequently purified by cation exchange chromatography on Sephadex CM-25 resin in water.[8]

$[Ru(tpy\text{-}PO_3Et_2)(OH_2))_3]^{2+}$. $[Ru(tpy\text{-}PO_3Et_2)(OH_2))_3]^{2+}$ was generated in situ from the oxalato precursor, [Ru(tpy-PO_3Et_2)(C_2O_4)-(OH_2)], by acid-promoted solvolysis in 0.1 M $HClO_4$ (eq 1). The solvolysis reaction was complete after 30 min as determined by UV−vis spectroscopy.

$$[Ru(tpy\text{-}PO_3Et_2)(C_2O_4)(OH_2)] + 2H^+ \rightarrow [Ru(tpy\text{-}PO_3Et_2)(OH_2)_3]^{2+} + H_2C_2O_4 \quad (1)$$

$[Ru(tpy\text{-}PO_3H_2)(OH_2)_3]^{2+}$(1) on Glass|ITO, Glass|ITO|TiO_2, or Glass|TiO_2. Stock solutions of the hydrolyzed, tris-aqua complex were prepared by heating [Ru(tpy-PO_3Et_2)$(C\text{-}_2O_4)(OH_2)$] in 1.0 M triflic acid at reflux for 15 h under argon. Stock solutions were stored under argon in the refrigerator until they were used.

Small portions of the reddish purple stock solution were diluted with 0.10 M triflic acid, and ITO electrodes, glass|ITO|TiO_2, or glass|TiO_2 slides were added to the solution for various soaking periods. Saturation coverage of the ITO electrodes was achieved in 2−3 h as monitored by the area under the cyclic voltammetric wave for the Ru(III/II) couple. This procedure resulted in ITO electrodes with maximum surface coverage of $3.8(5) \times 10^{-11}$ mol/cm^2.[9] These coverages are lower by a factor of ∼3 than coverages with $[Ru^{II}(tpy)(4,4'\text{-}(PO_3H_2)_2(bpy)(OH_2)]^{2+}$, presumably because of the presence of a single phosphonate group for surface binding. Saturation coverage on glass|TiO_2 was achieved in 7−8 h as determined by changes in the visible absorption spectrum at 500 nm (abs = 0.55). The extinction coefficient of the unphosphonated analog, $[Ru^{II}(tpy)(OH_2)_3]^{2+}$ (ϵ = 3450 M^{-1} cm^{-1}), was used to estimate maximum surface coverages of $1.5(3) \times 10^{-7}$ mol/cm^2.[8]

Measurements. Electrochemical experiments were conducted by using a CH Instruments 620b electrochemical analyzer in a three-electrode cell with a Pt auxiliary electrode and a Ag/AgCl reference electrode at −0.044 V relative to SCE. All potentials are cited versus SCE. pH-dependent cyclic voltammetric measurements were carried out in 0.05 M phosphate buffer solutions adjusted to 0.10 M ionic strength with $NaClO_4$. The electrocatalytic oxidation experiments were performed in 0.10 M $HClO_4$. Spectrophotometric experiments were carried out with a HP 8452 diode array spectrophotometer. Absorption versus time data were exported to Origin 7.5 for mathematical analysis.

Results and Discussion

Electrochemistry. Cyclic voltammograms (CV) of ITO electrodes with maximum surface coverages of $[Ru(tpy\text{-}PO_3H_2)(OH_2)_3]^{2+}$ (**1**) on fully loaded ITO surfaces ($\Gamma \approx 4 \times 10^{-11}$ mol/cm^2) at pH 1 show quasi-reversible, single-electron waves for the III/II and IV/III couples at 0.56 and 0.81 V and, for the two-electron VI/IV couple, at 1.00 V vs SCE. At a scan rate of 20 mV/s, the peak-to-peak separation between the oxidative and reductive waves (ΔE_p) was ∼0 for the (III/II) couple as expected for the surface-bound Ru(III/II) couple in eq 2 undergoing fast electron transfer.[9] By contrast, the ΔE_p values and wave shapes for the remaining couples are dependent on scan rate and the composition of the external solution in a complex way. These kinetic effects, which are currently under investigation, are caused by slow electron-transfer rates arising from proton-coupled electron transfer (PCET) and slow proton loss in couples involving oxo formation (eqs 3 and 4).[1,10]

$$ITO|[(HO)_2OP)tpy)Ru^{III}(OH_2)_3]^{3+} + e^- \rightarrow ITO|[(HO)_2OP)tpy)Ru^{II}(OH_2)_3]^{2+} \quad (2)$$

$$ITO|[((HO)_2OP)tpy)Ru^{IV}(O)(OH_2)_2]^{2+} + e^- + 2H^+ \rightarrow ITO|[((HO)_2OP)tpy)Ru^{III}(OH_2)_3]^{3+} \quad (3)$$

$$ITO|[((HO)_2OP)tpy)Ru^{VI}(O)_2(OH_2)]^{2+} + 2\,e^- + 2\,H^+ \rightarrow ITO|[((HO)_2OP)tpy)Ru^{IV}(O)(OH_2)_2]^{2+} \quad (4)$$

As can be seen in the CV of the surface-bound complex in Figure 1, a small amount of surface-bound μ-oxo dimer, glass|ITO|[$(OH)_2$OP)tpy)$(OH_2)_2Ru^{III}$−O−$Ru^{III}(OH_2)_2$(tpy-

(6) (a) Huang, J.-S.; Leung, S. K.-Y.; Zhou, Z.-Y.; Zhu, N.; Che, C. M. *Inorg. Chem*. **2005**, *44*, 3780−3788. (b) Mucientes, A. E.; Gabaldón, R. E.; Poblete, F. J.; Villarreal, S. *J. Phys. Org. Chem*. **2004**, *17*, 236−240. (c) Lam, W. W. Y.; Yiu, S.-M.; Yiu, D. T. Y.; Lau, T.-C.; Yip, W.-P.; Che, C.-M. *Inorg. Chem*. **2003**, 42, 8011−8018. (d) Yiu, D. T. Y.; Lee, M. F. W.; Lam, W. W. Y.; Lau, T.-C. *Inorg. Chem*. **2003**, *42*, 1225−1232. (e) Lebeau, E. L.; Meyer, T. J. *Inorg. Chem*. **1999**, *38*, 2174−2181. (f) Dovletoglou, A.; Meyer, T. J. *J. Am. Chem. Soc*. **1994**, *116*, 215−223.

(7) Argazzi, R.; Bignozzi, C. A.; Heimer, T. A.; Castellano, F. N.; Meyer, G. *J. Phys. Chem. B* **1997**, *101*, 2591−2597.

(8) Adeyemi, S. A.; Dovletoglou, A.; Guadalupe, A. R.; Meyer, T. J. *Inorg. Chem*. **1992**, *31*, 1375−1383.

(9) (a) The area under the CV wave was converted to surface coverage (Γ in mol/cm^2) according to the equation Γ = (area under CV wave)/*nFA*, where n is the number of electrons, *F* is Faraday's constant, and *A* is the area of the electrode in cm^2. (b) Bard, A. J.; Faulkner, L. R. *Electrochemical Methods: Fundamentals and Applications*, 2nd ed.; John Wiley: New York, 2001.

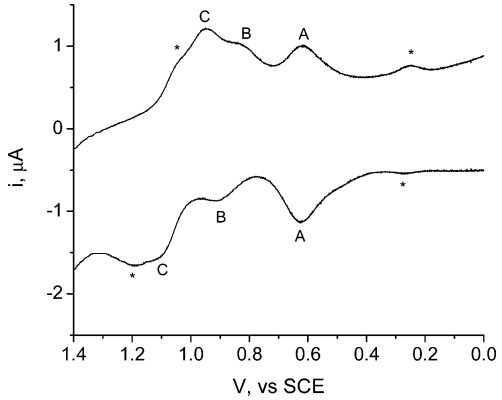

Figure 1. Cyclic voltammogram of **1** on glass|ITO at a surface coverage $\Gamma = 3.1 \times 10^{-11}$ mol/cm^2 in 0.10 M $HClO_4$ at 23 °C vs SCE at a scan rate of 0.020 V/s. Waves for the Ru(III/II) (A), Ru(IV/III) (B), and Ru(VI/IV) (C) couples are labeled. Waves marked with an asterisk (*) are from the μ-oxo dimer, $[(OH)_2(O)P)tpy)(OH_2)_2Ru^{III}-O-Ru^{III}(OH_2)_2(tpy(P(O)(OH)_2]^{4+}$, see text.

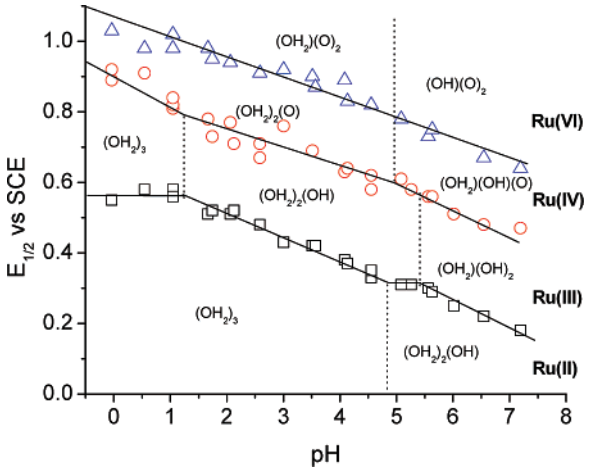

Figure 2. $E_{1/2}$ vs pH plots for **1** on glass|ITO in aqueous phosphate buffers at constant ionic strength (0.1 M) vs SCE at 23 °C. pH−potential regions of stability for the various oxidation states of the complex are labeled as Ru(II), Ru(III), etc. Compositions of the various oxidation state forms in the *trans*-H_2O, OH, and O ligands are indicated. For example, Ru(III) $(OH_2)_3$ corresponds to ITO|$((HO)_2OP)tpy)Ru^{III}(OH_2)_3^{3+}$. The vertical lines are approximate pK_a values.

$(PO(OH)_2]^{4+}$, also appears on the surface.[11a] This can be seen in the CV by the waves appearing at $E_{1/2} = 0.26$ and 1.10 V. These potentials coincide with those of the solution analog, $[(tpy)(OH_2)_2Ru^{III}-O-Ru^{III}(OH_2)_2(tpy)]^{4+}$.[11b] The formation and reactivity of the dimer on the ITO and TiO_2 surfaces is the subject of an ongoing investigation, and an initial communication has appeared.[11a]

The appearance of a two-electron wave for the *trans*-$[O{=}Ru^{VI}{=}O]^{2+} \rightarrow [Ru^{IV}{=}O]^{2+}$ couple is consistent with solution results showing that Ru(V) is unstable with respect to disproportionation at pH 1 with $E_{1/2}(Ru(V/IV)) > E_{1/2}(Ru(VI/V))$. The net reaction, $2Ru(V) \rightarrow [Ru^{IV}(tpy)(O)(OH_2)_2^{2+} + [Ru^{VI}(tpy)(O)_2(OH_2)^{2+}$, in spontaneous. Because the potential for oxidation of Ru(IV) is more positive than the oxidation of Ru(V). Once formed, Ru(V) undergoes further oxidation by electron transfer at the electrode and does not build up as an intermediate. This is the origin of the 2e$^-$ Ru(VI/IV) wave. The same behavior has been found for the related *trans*-dioxo complexes $[Ru^{VI}(bpy)_2(O)_2]^{2+}$,[11] $[Os^{VI}(bpy)_2(O)_2]^{2+}$,[12] $[Os^{VI}(phen)(O)_2(OH)_2]$, and $[Os^{VI}(tpy)(O)_2(OH)]^+$.[13]

Table 1. Comparison of $E_{1/2}$ Values for Solution, $Ru(tpy)(OH_2)_3^{2+}$, and Surface Couples Glass|ITO|$[(HO)_2OP)tpy)Ru^{II}(OH_2)_3]^{2+}$ (ITO) and Glass|ITO|$TiO_2-((HO)_2OP)tpy)Ru^{III}(H_2O)_3^{2+}$ (ITO|TiO_2) in Water at $I = 0.1$ vs SCE

Ru couple	solution[a]	glass|ITO[b]	glass|ITO|TiO_2[b]
$Ru^{III}(OH_2)_3^{3+}/Ru^{II}(OH_2)_3^{2+}$	0.55	0.61	0.60
$Ru^{IV}(O)(OH_2)_2^{2+}/Ru^{III}(OH_2)_3^{2+}$	0.95	0.86	0.84
$Ru^{VI}(O)_2(OH_2)^{2+}/Ru^{IV}(O)(OH_2)_2^{2+}$	1.11	1.04	1.02

[a] From ref 8. Measured at an "activated" glassy-carbon-disk electrode, 0.1 M $HClO_4$, $I = 0.10$ M, 100 mV/s. [b] This work. Pt counter electrode vs SCE at a scan rate of 20 mV/s.

Table 2. Comparison of pK_a Values for Solution and Surface Couples

complex	solution	ITO
	$Ru(tpy)(OH_2)_3^{2+}$	
p$K_{a,1}$	5.3	4.8 ± 0.3
p$K_{a,2}$	>8	>8
	$Ru(tpy)(OH_2)_3^{3+}$	
p$K_{a,1}$	2.1	1.2 ± 0.2
p$K_{a,2}$	4.6	5.4 ± 0.3
	$Ru(tpy)(O)(OH_2)_2^{2+}$	
p$K_{a,1}$	5.2	5.0 ± 0.5
p$K_{a,2}$	>8	>8
	$Ru(tpy)(O)_2(OH_2)^{2+}$	
p$K_{a,1}$	5.2	5.0 ± 0.5
p$K_{a,2}$	>8	>8

The inversion in potentials that leads to disproportionation is a consequence of two effects. One is PCET with loss of both an electron and proton between adjacent couples, for example, $[Ru^{IV}(tpy)(O)(OH_2)_2^{2+}/[Ru^{III}(tpy)(OH)(OH_2)_2^{2+}$ and $[Ru^{III}(tpy)(OH)(OH_2)_2^{2+}/[Ru^{II}(tpy)(OH_2)_3^{2+}$. This results in no charge build up for the higher-oxidation state couple. The second effect is electronic stabilization of *trans*-$[O{=}M^{VI}{=}O]^{2+}$ resulting from the *trans*-dioxo interaction.[6,11,13,14]

Kinetic nuances for couples higher than Ru(III/II), arising from scan rate and solution composition effects, also appear for couples on glass|ITO and on glass|ITO|TiO_2 surfaces. However, waves for all three couples, Ru(III/II), Ru(IV/III), and Ru(VI/IV), were observed at the same $E_{1/2}$ values within experimental error (Tables 1 and 2). In addition, the pH dependence (pH 0−7.2) for the three couples on glass|ITO, Figure 2, are very similar to the analogous solution values, which demonstrate that the surface bound complexes have comparable pK_a values. The acid dissociation constants are

(10) (a) Roth, J. P.; Yoder, J. C.; Won, T. J.; Mayer, J. M. *Science*, **2001**, *249*, 2524−2526. (b) Hammes-Schiffer, S. *Acc. Chem. Res.* **2001**, *34*, 273−281. (c) Cukier, R. I.; Nocera, D. G. *Annu. Rev. Phys. Chem.* **1998**, *49*, 337−369. (d) Che, C. M.; Lau, K.; Lau, T. C.; Poon, C. K. *J. Am. Chem. Soc.* **1990**, *112*, 5176−5181. (d) Thorp, H. H.; Sarneski, J. E.; Brudvig, G. W.; Crabtree, R. H. *J. Am. Chem. Soc.* **1989**, *111*, 9249−9250. (f) Binstead, R. A.; Moyer, B. A.; Samuels, G. J.; Meyer, T. J. *J. Am. Chem. Soc.* **1981**, *103*, 2897−2899.

(11) (a) Liu, F.; Cardolaccia, T.; Hornstein, B. J.; Schoonover, J. R.; Meyer, T. J. J. Am. Chem. Soc. **2007**, *129*, 2446−2447. (b) Lebeau, E. L.; Adeyemi, S. A.; Meyer, T. J. *Inorg. Chem.* **1998**, *37*, 6476−6484.

(12) (a) Dobson, J. C.; Meyer, T. J. *Inorg. Chem.* **1988**, *27*, 3283−3291. (b) Dobson, J. C.; Takeuchi, K. J.; Pipes, D. W.; Geselowitz, D. A.; Meyer, T. J. *Inorg. Chem.* **1986**, *25*, 2357.

(13) Pipes, D. W.; Meyer, T. J. *Inorg. Chem.* **1986**, *25*, 4042−4050.

(14) Huynh, M. H. V.; Meyer *Coord. Chem. Rev.* **2007**, submitted.

derived from the dotted vertical lines on the potential−pH diagram in Figure 2 and are compared to the solution values in Table 2. Given the sensitivity of these couples to substituent changes at the ligands the agreement in potentials and pK_a values, between solution and surface couples, where exchange is made of −H for −P(O)(OH)$_2$ at the 6″ position on tpy, may be partly fortuitous.[1,15] Nonetheless, it is an important result because it shows that the thermodynamic redox and acid−base properties of the complex are retained on the oxide surfaces.

Reactivity on TiO_2. Characterization. The electrochemical results show that the higher oxidation states Ru(IV) and Ru(VI) are accessible on the electrode surfaces. As a means for developing strongly oxidizing surfaces, we have explored the oxidative reactivity of glass|ITO|TiO_2−(((HO)$_2$OP)tpy)-$Ru^{VI}(O)_2(OH_2)^{2+}$ within high surface area, ∼10 μm TiO_2 films toward benzyl alcohol. As exploited in an earlier study,[5] the use of optically transparent nanoparticle films allows quantitative surface reactivity studies to be conducted with use of conventional UV−vis spectrophotometry.[16]

To assess reactivity, glass|TiO_2−((HO)$_2$OP)tpy)$Ru^{VI}(O)_2$-$(OH_2)^{2+}$ (glass|TiO_2−$Ru^{VI}(O)_2^{2+}$) was generated from glass|TiO_2−$Ru^{II}(OH_2)_3^{2+}$ by placing a Ru-coated film in a solution containing 0.02 M Ce(IV) in 0.10 M $HClO_4$. Oxidation is accompanied by the expected color change from purple to yellow and the appearance of an absorption feature at 410 nm ($\epsilon \sim 3{,}700\ M^{-1}cm^{-1}$) that is characteristic of Ru^{VI}-$(O)_2^{2+}$(Figure S1 in Supporting Information). UV−vis measurements of the oxidized films were made in fresh 0.10 M $HClO_4$ solutions and were used to estimate the amount of $Ru^{VI}(O)_2^{2+}$ present in the films. As with the calculation of adsorbed Ru(II) (see the Experimental Section), the extinction coefficient for the unphosphonated analog was used in this calculation. A comparison of surface coverage before and after oxidation shows that there is a negligible loss of Ru from the surface over the course of the Ru(II) → Ru(VI) reaction.

In addition to spectroscopic characterization, the number of oxidizing equivalents was confirmed by a titration with hydroquinone. This experiment was carried out as described previously[5] with spectrophotometric analysis giving 4.0 ± 0.6 equiv, which is consistent with the reduction of Ru(VI) to Ru(II) (eq 5). More specifically, the oxidized Ru(VI) film was exposed to a standard aqueous solution of hydroquinone at pH 1. After 30 min, the film was removed, and the concentration of the benzoquinone produced was determined by its UV absorption at 248 nm ($\epsilon_{248} = 20\ 700\ cm^{-1}\ M^{-1}$).[17] The amount of benzoquinone produced was consistent with eq 5 and with the spectrophotometrically determined concentration of Ru(VI) in the TiO_2 film.

Oxidation of Benzyl Alcohol. To assess the impact of surface binding on reactivity, we undertook a kinetic investigation of the oxidation of benzyl alcohol in acetonitrile. In solution, the use of acetonitrile prevents the formation of oxo-bridged dimers that complicate the kinetics of benzyl alcohol oxidation. In an earlier detailed mechanistic study, oxidation of benzyl alcohol by *trans*-$[Ru^{VI}(tpy)(O)_2(H_2O)]^{2+}$ was investigated in both water and acetonitrile as solvents. In dry acetonitrile, the dominant forms of Ru(VI) and Ru(IV) are *trans*-$[Ru^{VI}(tpy)(O)_2(NCMe)]^{2+}$ and $[Ru^{IV}(tpy)(O)(NCMe)_2^{2+}$,[8] and we assume the same compositions on the surface, glass|TiO_2−((HO)$_2$OP)tpy)$Ru^{VI}(O)_2(NCCH_3)^{2+}$ (glass|TiO_2−$Ru^{VI}(O)_2^{2+}$) and glass|TiO_2−((HO)$_2$OP)tpy)-$Ru^{IV}(O)(NCCH_3)_2^{2+}$ (glass|TiO_2−$Ru^{IV}(O)(NCMe)_2^{2+}$).

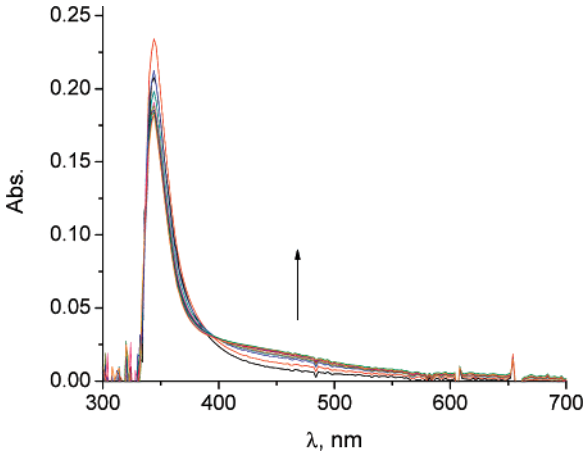

Figure 3. UV−vis absorption spectra at various times for the reaction between glass|TiO_2−$Ru^{VI}(O)_2^{2+}$ and benzyl alcohol (3.84 mM) in acetonitrile at 23 °C. Spectra were recorded at 12 s intervals. The increase at 450 nm is the result of the appearance of Ru(II).

$$\text{glass}|TiO_2-Ru^{VI}(O)_2^{2+} + 2HOC_6H_4OH \rightarrow \text{glass}|TiO_2-Ru^{II}(H_2O)_2^{2+} + 2OC_6H_4O \quad (5)$$

Films of glass|TiO_2−((HO)$_2$OP)tpy)$Ru^{VI}(O)_2(NCCH_3)^{2+}$ were prepared by oxidization of Ru(II) films with 0.02 M Ce(IV) in 0.10 M $HClO_4$. These were made as described above. After they were soaked for 5 min in the Ce(IV) solution, the films were removed, rinsed with water, then rinsed with dry acetonitrile, and finally placed in a cuvette containing a stir bar and dry acetonitrile. The films were stirred in acetonitrile for 5 min before 0.05−0.5 mL of a freshly prepared benzyl alcohol solution in acetonitrile was added. Upon addition of benzyl alcohol, stepwise reactions occur which are well separated in time. The first involves reduction of Ru(VI) to Ru(IV), followed by the slower reduction of Ru(IV) to Ru(II). A UV−vis spectral trace obtained for glass|TiO_2−$Ru^{VI}(O)_2^{2+}$ after the addition of benzyl alcohol in dry acetonitrile is shown in Figure 3. The reduction of Ru(VI) is rapid and difficult to monitor because of the low absorptivity at its absorption maximum at 410 nm.[13] The rapid, Ru(VI) → Ru(IV) step was studied at low concentrations of benzyl alcohol (0.05−0.5 mM), and the Ru(IV) → Ru(II) step was studied at higher concentrations (0.05−9.6 mM).

Absorbance−time traces for the first step, monitored in the range of 344−370 nm, followed first-order kinetics.

(15) Masllorens, E.; Rodriques, M.; Romero, I.; Roglans, A.; Parella, T.; Benet-Buchholz, J.; Poyatos, M.; Llobet, A. *J. Am. Chem. Soc.* **2006**, *128*, 5306−5307.

(16) Kalyanasundaram, K.; Gratzel, M. *Coord. Chem. Rev.* **1998**, *77*, 347−414.

(17) Binstead, R. A.; McGuire, M. E.; Dovletoglou, A.; Seok, W. K.; Roeker, L. E.; Meyer, T. J. *J. Am Chem. Soc.* **1992**, *114*, 173−186.

Absorbance−time traces for the slower reaction between benzyl alcohol and $Ru^{IV}{=}O^{2+}$ were monitored at 450 nm, the visible λ_{max} for the final glass|TiO_2-((HO)$_2$OP)tpy)Ru^{II}-$(NCCH_3)_3^{2+}$ product. Absorbance−time traces were nonexponential at this wavelength but could be fit to the double-exponential function, $\Delta A = A_1 \exp(-k_1 t) + A_2 \exp(-k_2 t)$, where ΔA is the absorbance change at time t. Typical plots of absorbance−time traces for both reactions are provided in Supporting Information, Figures S2 and S3.

The observed rate constant for reduction of $Ru^{VI}(O)_2^{2+}$, $k_{VI,obs}$, is linearly dependent on the concentration of benzyl alcohol, [BzOH], Figure S4, consistent with the rate law, $-d[Ru^{VI}(O)_2^{2+}]/dt = k_{VI}P[Ru^{VI}(O)_2^{2+}][BzOH]$, and the reaction in eq 6. This result is consistent with the earlier solution results. In this expression, P is the partition coefficient describing the distribution of benzyl alcohol between the film and solution in acetonitrile with, $P = [BzOH]_{film}/[BzOH]_{solution}$. From the slope of a plot of $k_{VI,obs}$ versus [BzOH], $k_{VI}P = 62 \pm 5\ M^{-1}\ s^{-1}$. As shown in Figure S4, these data also reveal a small nonzero intercept that is caused by the reaction of $[Ru^{VI}(O)_2]^{2+}$ with acetonitrile ($k_{solv} = 1.8 \times 10^{-3}\ s^{-1}$). A similar value for background oxidation of acetonitrile was reported previously for $[Ru^{VI}(tpy)(O)_2(NCMe)]^{2+}$.[6e]

The rate constant for benzyl alcohol oxidation by $[Ru^{VI}(tpy)(O)_2(NCMe)]^{2+}$ in acetonitrile is $k = 67 \pm 3\ M^{-1}\ s^{-1}$, close to $k_{VI}P = 62 \pm 5\ M^{-1}\ s^{-1}$ on the surface. Given the other indicators suggesting retention of reactivity on the surface, this result implies that the partition coefficient, P, is not greatly different from 1.[6e]

$$\text{glass}|TiO_2-Ru^{VI}(O)_2(NCMe)^{2+} + PhCH_2OH + 2CH_3CN \rightarrow \text{glass}|TiO_2-Ru^{IV}(O)(NCMe)_2^{2+} + PhCHO + H_2O \quad (6)$$

On the basis of a detailed mechanistic analysis, including ^{18}O labeling, the mechanism proposed for oxidation of benzyl alcohol by *trans*-$[Ru^{VI}(tpy)(O)_2(NCMe)]^{2+}$ in solution was rate-limiting C−H insertion to give the coordinated aldehyde hydrate, $[Ru^{IV}-O(H)CH(OH)Ph]^{2+}$.[18] Insertion is followed by rapid release of the hydrate to give $[Ru^{IV}(tpy)(O)(NCMe)_3]^{2+}$ with subsequent dehydration of the hydrate to give the aldehyde, $PhC(OH)_2H \rightarrow PhCHO + H_2O$.

Reactivity toward benzyl alcohol is also maintained on glass|$TiO_2-Ru^{IV}(O)^{2+}$ in acetonitrile. As noted above, the kinetics of appearance of Ru(II) are biexponential with absorption−time plots (ΔA vs t) at 450 nm varying as $A_1 \exp(-k_1 t) + A_2 \exp(-k_2 t)$, consistent with dynamic overlap between oxidation and solvolysis. In the treatment of the absorbance−time decay data, k_1 was independent of added alcohol, while k_2 varied linearly with alcohol concentration consistent with the mechanism in eqs 7 and 8. A related mechanism was identified for oxidation of benzyl alcohol by $[Ru^{IV}(tpy)(O)(NCMe)_3]^{2+}$ in acetonitrile, where it was concluded that C−H insertion was also involved at the Ru(IV) to Ru(II) stage to give the bound Ru(II) aldehyde hydrate, $[Ru^{II}(HOCH(OH)Ph]^{2+}$.[19]

Scheme 1

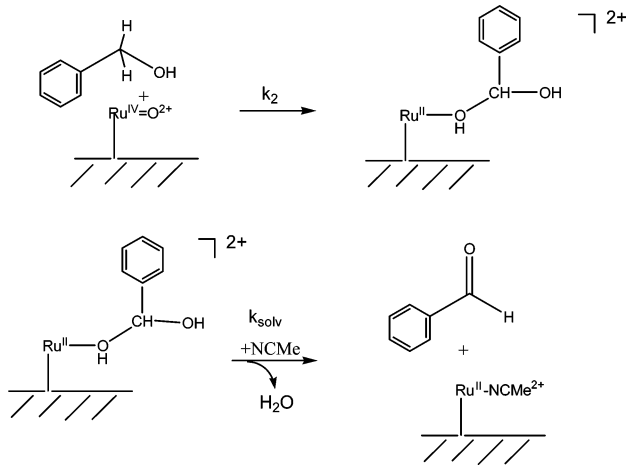

$$\text{glass}|TiO_2-Ru^{IV}(O)(NCMe)_2^{2+} + PhCH_2OH \rightarrow \text{glass}|TiO_2-Ru^{II}(HOCH(OH)Ph)(NCMe)_2]^{2+} \quad (7)$$

$$\text{glass}|TiO_2-Ru^{II}\text{-}(HOCH(OH)Ph)](NCMe)_2]^{2+} + NCMe \rightarrow \text{glass}|TiO_2-Ru^{II}(NCMe)_3^{2+} + PhCHO + H_2O \quad (8)$$

For the alcohol dependent term, $-d[Ru^{IV}(O)^{2+}]/dt = k_{IV,obs}[Ru^{IV}(O)^{2+}][BzOH]$ with $k_{IV,obs} = k_{IV}P'[BzOH]$ with $k_{IV}P' = 1.2 \pm 0.2\ M^{-1}\ s^{-1}$, where P' is the partition coefficient with Ru^{IV} on the surface, Figure S5. For the surface−solution comparison for Ru(IV), this value is remarkably near $k = 1.5\ M^{-1}\ s^{-1}$ for oxidation of the alcohol by $[Ru^{IV}(tpy)(O)(NCMe)_3]^{2+}$ under the same conditions in acetonitrile. As noted above, the alcohol-independent term in the biexponential kinetics arises from solvolysis of the coordinated aldehyde hydrate. It occurs with $k_1 = 7 \times 10^{-4}\ s^{-1}$ to give glass|$TiO_2-Ru^{II}(NCMe)_3^{2+}$.[5,11]

The implied mechanism for surface oxidation of benzyl alcohol by Ru(IV) followed by solvolysis is illustrated in Scheme 1.

Electrocatalysis. The electrocatalytic behavior of the surface glass|ITO|$TiO_2-[((HO)_2OP)tpy)Ru^{VI}(O)_2(OH_2)]^{2+}$/$Ru^{IV}(O)(OH_2)_2^{2+}$ couple was of special interest. To explore this behavior, a series of electrocatalytic experiments was undertaken in 0.10 M aqueous $HClO_4$ in the presence of varying amounts of benzyl alcohol.

Linear sweep voltammograms and control experiments for glass|ITO|$TiO_2-Ru^{II}(H_2O)_3^{2+}$ in the presence of benzyl alcohol are shown in Figure 4. These results reveal a current enhancement of >7 at the peak potential for the Ru(VI)/Ru(IV) wave in the presence of 0.090 M benzyl alcohol. Because of problems with the current background on ITO, limiting plateau currents were not observed, and the extent of catalysis was arbitrarily taken as the current enhancement at 1.54 V.

(18) Lebeau, E. L.; Meyer, T. J. *Inorg. Chem.* **1999**, *38*, 2174−2181.

(19) Roecker, L.; Meyer, T. J. *J. Am. Chem. Soc.* **1987**, *109*, 746−754.

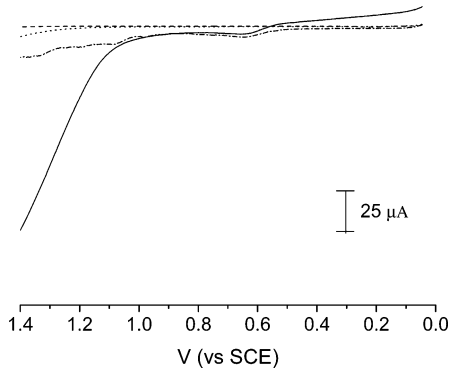

Figure 4. Linear sweep voltammograms recorded at 0.010 V/s in 0.1 M $HClO_4$ for (a) (---) blank glass|ITO|TiO_2 (b) (▪▪▪) blank glass|ITO|TiO_2 in 90 mM benzyl alcohol, (c) (-▪-▪-) glass|ITO|TiO_2−((HO)$_2$OP)tpy)Ru^{III}-$(H_2O)_3^{2+}$, and (d) (—) glass|ITO|TiO_2−((HO)$_2$OP)tpy)$Ru^{III}(H_2O)_3^{2+}$ in 90 mM benzyl alcohol.

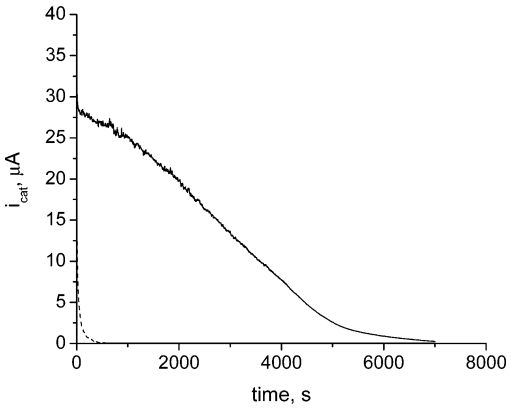

Figure 5. Variation of i_{cat} vs time for the electrocatalytic oxidation of benzyl alcohol by glass|TiO_2−$Ru^{VI}(O)_2^{2+}$. Conditions: E = 1.54 V (vs SCE), [BzOH] = 0.20 M, 0.10 M $HClO_4$, 23 °C. The dashed line is the same reaction carried out in the absence of benzyl alcohol.

For a rate-limiting catalytic EC mechanism, the catalytic current is described by eq 9 when the chemical step is irreversible.[9b,20] In eq 9, D is the diffusion coefficient for benzyl alcohol in centimeters squared per second (cm^2/s), n the electrochemical stoichiometry, [BzOH] is the concentration of benzyl alcohol in moles per cubic centimeter (mol/cm^3), F is the Faraday constant, A is the electrode area in centimeters squared (cm^2), [Ru] is the (fixed) surface concentration of Ru in moles per sqaure centimeter (mol/cm^2) in the film, and once again, P is the partition coefficient for benzyl alcohol between the film and external solution.

$$i_{cat} = (nFA)[\mathrm{Ru}](k_{cat}DP[\mathrm{BzOH}])^{1/2} \quad (9)$$

From the zero-intercept and linearity of the plot shown in Figure S6 (r = 0.98), i_{cat} (taken as the current at 1.54 V) was found to vary with $[BzOH]^{1/2}$, consistent with eq 9, Figure S6.[20] An accurate study of the dependence of i_{cat} on surface loading of Ru (in mol/cm^{-2}) was precluded by formation of the μ-oxo dimer at high surface loadings. Assumption of first order behavior in Ru seems warranted by the results of numerous studies on the oxidation of benzyl alcohol and other reductants by ruthenium−oxo complexes in solution.[1,21,22]

To eliminate the dependence of the apparent second-order rate constant (k_{cat}) on the diffusion coefficient (D) and effective surface area of each Ru-coated electrode (A), eq 9 was normalized with the expression for peak current in the absence of benzyl alcohol described by the Randles−Sevcik equation, eq 10, where ν is the scan rate (V/s) and i_p is the peak current for the wave for the catalyst couple in the absence of benzyl alcohol.[23] Dividing and rearranging it

$$i_p = (2.69 \times 10^5)n^{3/2}AD^{1/2}[\mathrm{Ru}]\nu^{1/2} \quad (10)$$

provides the useful expression in eq 11.

$$\frac{i_{cat}}{i_p} = \left(\frac{k_{cat}}{7.77n\nu}P[\mathrm{BzOH}]\right)^{1/2} \quad (11)$$

A plot of i_{cat}/i_p versus $[BzOH]^{1/2}$ is linear (r = 0.97, Figure S7) and yields the product $k_{cat}P$ with $k_{cat}P = 62 \pm 5\ M^{-1}\ s^{-1}$. This value is within experimental error of the value observed directly in acetontrile in the spectrophotometric study described in the previous section. For the oxidation of benzyl alcohol by $[Ru^{VI}(tpy)(O)_2(OH_2)]^{2+}$ under the same conditions in 0.10 M aqueous $HClO_4$, $k_{VI} = 13\ M^{-1}\ s^{-1}$.[6e] The enhancement of reactivity on the surface in this case may reflect in part a greater partitioning of benzyl alcohol into the film in water with $P > 1$.

The stability of the surface catalyst over extended electrolysis periods was also investigated. In these experiments, the electrode potential was stepped to 1.54 V, past the peak potential for the Ru(VI)/(IV) wave at 1.04 V (vs SCE), and held for extended periods. In one experiment with [BzOH] = 0.20 M, electrolysis continued for ~2 h until the catalytic current approached 0. Integration of the i_{cat} versus t curve, Figure 5, showed that 130 ± 20 (n = 2) turnovers had occurred, based solely on the amount of current passed. While attempts to characterize the catalyst at the end of the electrolysis were not made, this result is similar to one obtained earlier from a polymer/film Ru(VI) system in which catalytic activity is also lost over extended electrolysis periods.[22b]

The addition of fresh benzyl alcohol to the reaction cell resulted in no significant recovery of catalytic current. Spectral and electrochemical measurements point to deactivation by a combination of partial desorption and a change in the chemical nature of the surface complex as reported

(20) Kutner, W.; Meyer, T. J.; Murray, R. W. *J. Electroanal. Chem.* **1985**, *195*, 375−394.

(21) (a) Lebeau, E. L.; Meyer, T. J. *Inorg. Chem.* **1999**, *38*, 2174−2181. (b) Yiu, D. T. Y.; Lee, M. F. W.; Lam, W. W. Y.; Lau, T.-C. *Inorg. Chem.* **2003**, *42*, 1225−1232. (c) Dovletoglou, A.; Meyer, T. J. *J. Am. Chem. Soc.* **1994**, *116*, 215−223. (d) Lam, W. W. Y.; Yiu, S.-M.; Yiu, D. T. Y.; Lau, T.-C.; Yip, W. P.; Che, C.-M. *Inorg. Chem.* **2003**, *42*, 8011−8018.

(22) (a) Sens, C.; Rodriguez, M.; Romero, I.; Llobet, A. *Inorg. Chem.* **2003**, *42*, 8385−8394. (b) Moss, J. A.; Leasure, R. M.; Meyer, T. J. *Inorg. Chem.* **2000**, *39*, 1052−1058. (c) Catalano, V. J.; Heck, R. A.; Immos, C. E.; Ohman, A.; Hill, M. G. *Inorg. Chem.* **1998**, *37*, 2150−2157. (d) Gerli, A.; Reedijk, J.; Lakin, M. T.; Spek, A. L. *Inorg. Chem.* **1995**, *34*, 1836−1843. (e) Guadalupe, A. R.; Chen, X. C.; Sullivan, B. P.; Meyer, T. J. *Inorg. Chem.* **1993**, *32*, 5502−5512.

(23) Galus, Z. *Fundamentals of Electrochemical Analysis*; Halsted Press: New York, 1976.

earlier for other Ru−oxo complexes.[11b,22e,24,25] Further investigation of catalyst deactivation is ongoing.

Conclusions

We have demonstrated that phosphonated ruthenium trisaqua complex, **1**, either adsorbed to an ITO surface or incorporated into a TiO_2 film, maintains its redox reactivity after attachment. Surface potentials, pH dependences, and pK_a values are comparable to those for $[Ru^{II}(tpy)(H_2O)_2]^{2+}$ in solution. Kinetic studies on the oxidation of benzyl alcohol to benzaldehyde by glass|ITO|TiO_2−((HO)$_2$OP)tpy)-$Ru^{VI}(O)_2(NCMe)^{2+}$in acetonitrile are also consistent with solution results with stepwise $Ru^{VI} \rightarrow Ru^{IV}$ oxidation of benzyl alcohol to benzaldehye, followed by slower $Ru^{IV} \rightarrow Ru^{II}$ oxidation to benzaldehye and solvolysis of coordinated benzaldehyde hydrate giving, ultimately, glass|ITO|TiO_2−((HO)$_2$OP)tpy)$Ru^{II}(NCMe)_3^{2+}$. Under electrocatalytic conditions in water, the oxidation of benzyl alcohol occurs through ∼130 (2e$^-$) turnovers with catalysis terminated by partial loss from the electrode surface and change in chemical state of the adsorbed catalyst.

Acknowledgment. We thank Fabrice Odobel for providing a sample of the phosphonated tpy ligand. Funding for this research was provided by Los Alamos National Laboratory (Laboratory Directed Research and Development Grant 20020222).

Supporting Information Available: Figures showing the spectrum of glass|TiO_2|$Ru^{IV}(H_2O_3Ptpy)(O)_2(NCMe)^{2+}$ in acetonitrile, the absorbance at 370 nm versus time plots for the reaction of glass|TiO_2|$Ru^{VI}(H_2O_3Ptpy)(O)_2(NCMe)^{2+}$ with 1.0×10^{-4} M benzyl alcohol in acetonitrile, the absorbance at 450 nm versus time for the reaction of glass|TiO_2|$Ru^{IV}(H_2O_3Ptpy)(O)(NCMe)_2^{2+}$ with 4.81×10^{-3} mM benzyl alcohol in acetonitrile, the plot of $k_{VI,obs}$ versus benzyl alcohol concentration, the plot of $k_{IV,obs}$ versus benzyl alcohol concentration in acetonitrile, the plot of catalytic current versus the square root of benzyl alcohol concentration for glass|ITO|TiO_2−$[((HO)_2OP)tpy)Ru^{VI}(O)_2(OH_2)]^{2+}$, and the plot of i_{cat}/i_p versus the square root of benzyl alcohol concentration for the electrocatalytic oxidation of benzyl alcohol carried out in 0.10 M $HClO_4$. This material is available free of charge via the Internet at http://pubs.acs.org.

IC0700506

(24) Geneste, F.; Moinet, C.; Ababou-Girard, S.; Solal, F. *Inorg. Chem.* **2005**, *44*, 4366−4371.
(25) McHatton, R. C.; Anson, F. C. *Inorg. Chem.* **1984**, *23*, 3935−3942.